

Finally, Figure 4.15 compares the mechanical and electrochemical properties of current ICMs²¹⁰⁻²²² and PEO-Kevlar LBL membranes. For high-power batteries, ionic conductivity of at least 10^{-3} S/cm is required to lower internal resistance, the area where is shaded with light green color. So far only liquid or gel-type electrolytes are able to achieve this level of performance, and it's the reason why they are currently the most commonly implemented electrolytes in portable electronic devices. Porous polymer separator incorporated with liquid electrolytes, PMMA and PAN-based, and PVdF-based separators are in this category. However, lack of mechanical stability makes them suffer from degradation and poor durability. To achieve dendrite-free in high-power-density lithium metal batteries, not only high ionic conductivity is required, the electrolyte or separator needs to be able to provide a compression force to the dendrites. From the numerical simulation done by Monroe et al, the Young's modulus and shear modulus of electrolyte or separator material need to be high enough to suppress dendrites from growing. The required mechanical strength is shaded in orange color. Current porous polymer separator or gel-type polymer-based electrolytes are orders too weak to achieve this goal. Solid-state electrolytes generally have very high ionic conductivity and mechanical stiffness, but too high the modulus results in too high the stiffness and lack of freedom of design. These electrolytes are harder to be implemented into all kinds of cell geometry. Finally, although PEO-based electrolytes generally exhibit lower ionic conductivity and low mechanical strength, with the incorporation of inorganic or organic fillers actually make them orders stronger without sacrificing electrochemical performance.

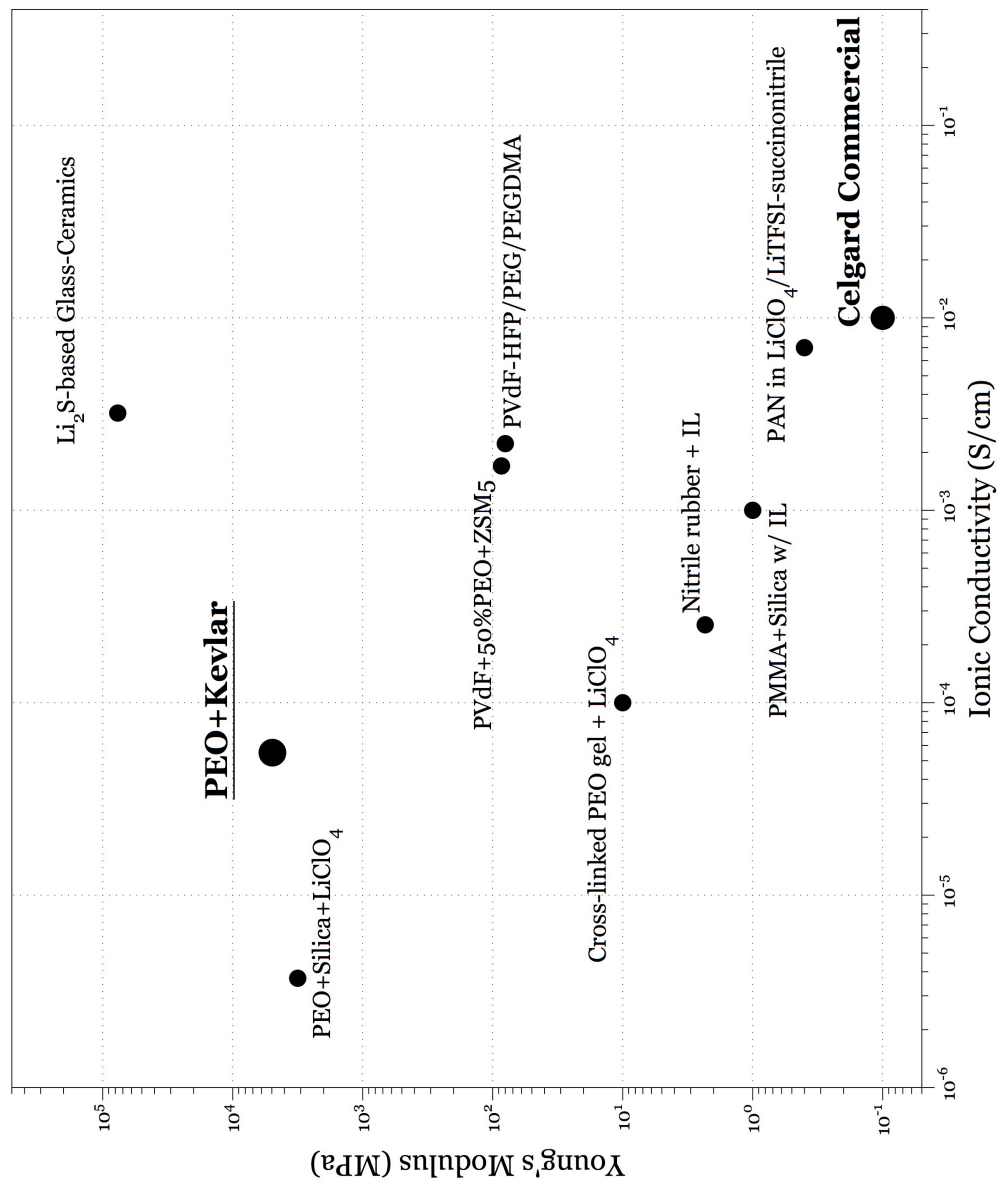


Figure 4.15 Common lithium battery electrolytes versus their mechanical modulus.

4.7 Dendrite Suppression

Dendrite growth in lithium metal batteries during charging cycle was simulated by electrodeposition of copper in electrochemical cell setup using copper as both anode and cathode. Copper was used instead of lithium in the experiments due to ease of investigation and its stability in room temperature and atmosphere. Bare copper electrodes with active surface area of 1 cm^2 were prepared and cleaned with acetone and DI water before use. 0.1M of copper chloride (CuCl_2) in DMSO solvent was prepared and used as electrolyte to prevent hydrogen evolution during deposition process. Current density was controlled by varying potential and distance between positive and negative electrodes. PEO-Kevlar membranes were deposited on copper anodes to cover the whole active area. Different numbers of bilayers were deposited to study the relationship between the dendrite formation and membrane thickness. Also, different current densities were used to drive copper ions to see the effectiveness of dendrite suppression by PEO-Kevlar membranes.

To more precisely compare the dendrite growth environment to actual situation in lithium batteries, a commercial Apple battery pack for 15" Unibody Macbook Pro was selected as the comparing model. The Apple battery pack has rated energy of 50 Whr, which is equivalent to 180 kilojoules. By the charge-discharge curves obtained from our battery tester, the Apple battery pack has an average voltage around 3.7 V, which suggests that LiCoO_2 chemistry is likely the one being implemented. The capacity of the battery pack can then be calculated to be 13.514 Ah. The dimensions of cathodes and anodes inside battery pack give the total active area of $6,006 \text{ cm}^2$, which ultimately gives

the current density of 2.25 mA/cm^2 , if charged with 1C rate (fully charge a battery in one hour). In daily life when the battery is mounted to the laptop computer, the charge rate is normally C/4 to C/3, so the current density in actual charging step will be in the range from 0.5 to 0.75 mA/cm^2 , with total charge transfer of 8.1 C (Coulomb) per Centimeter Square.

Since dendrites start to form when the current density is high, and we intended to investigate to what extent can PEO-Kevlar membrane effectively suppress dendrites from forming, current densities used in this study were all higher than current density observed at 1C rate. Figure 4.16 shows the surface SEM images of (A) bare copper, (B) [PEO-Kevlar]₁₀, and (C) [PEO-Kevlar]₂₀ anodes after deposition under high current density. 7.5 mA/cm^2 of current density was used to drive copper ions to the electrode surface, which can be viewed as charging an Apple laptop battery at a little bit higher than 3C rate. The total charge transferred was controlled at 2 C (Coulomb). Fluffy dendrites could be found on bare electrode (4.16(A)), as there was no constraint to limit dendrites from growing. On the electrode with 10 bilayers of PEO-Kevlar, although dendrites still grew vigorously, they were not as fluffy and seemed to lie flat on the electrode surface as in figure 4.16(B). Even though the thickness of [PEO-Kevlar]₁₀ was only about 100-130 nm, substantial effects on dendrite formation could already be seen. Dramatic dendrite morphology change could be found in 4.16(C), when 20 bilayers of PEO-Kevlar were deposited on the copper electrode. After 2 C of deposition under high current density, the dendrites were formed as "buds" on the electrode surface with very high density. The size of these "buds" was much smaller than fern-like dendrites. This is

a good indication that, with thicker PEO-Kevlar film on top of the electrode, and with the compressive force provided by PEO-Kevlar, copper was deposited evenly on the whole surface to form smaller "buds" instead of dramatically increasing the size of certain ones to form bigger structures to eventually short the circuit. This transformation could contribute to delaying dendrites from reaching the opposite electrode and extend life cycle of lithium metal batteries.

To further examine the stability of PEO-Kevlar membranes under sudden current density hike, a bare copper and a [PEO-Kevlar]₂₀ were put to test under 11.3 mA/cm² of current density (about 5C charging rate). At this rate, one could fully charge a lithium battery in about 12 minutes if the battery could handle it, or kill a lithium metal battery in the same amount of time if no better ICMs were created. Although only 0.5 C of charges were driven to the electrode in this experiment, a dendrite layer that was much thicker and denser than 4.16(A) could be found on bare copper surface (Figure 4.17 (A-C)). With the amount and size of these dendrites, one could imagine seeing them accumulating in commercial separator pores so fast, that the internal circuit was shorted in no time, especially the opposite electrode is on average only about 25 μm away. On the other hand, under the same current density and amount of charge transfer, [PEO-Kevlar]₂₀ showed exceptional dendrite confinement even though the thickness of the membrane is only roughly 280 nm. In Figure 4.17(D-F), copper dendrites were mostly still in bud-like form throughout the surface, with some random fern-like structures laying on the surface. The close-up image (4.17(F)) showed clearly that these bigger dendrites were still trapped under PEO-Kevlar membrane. So this set experiment suggested that PEO-Kevlar

could not only limit the growth of dendrites, but also provide an extra layer of protection to the battery in the case of power surge due to management failure or what ever reason during the charging process.

Lastly, long-time charging with lower current density was investigated between a bare copper electrode and a [PEO-Kevlar]₅₀ electrode. As calculated earlier, per unit area of electrode surface in Apple battery undergoes 8.1 C of charge transfer. To deposit same amount of copper atoms on the anodes, 20 C of charge were driven to the electrodes under current density of 2.75 mA/cm². On bare copper electrode, thick and dense copper layer seen in electroplating could be found (Figure 4.18 (A-C)). Instead of feather or fern-like structure, copper deposited at lower current density has different morphology, but this does not prevent the battery cells from failing because these metal deposits could still reach the opposite electrode through the pores, as demonstrated earlier in Figure 4.2 and 4.4. Conversely, and surprisingly, under the same deposition parameter, huge amount of sphere-shaped structures were found on [PEO-Kevlar]₅₀ electrode (Figure 4.18(D-F)). These are not copper or polymer microparticles but copper dendrites confined inside PEO-Kevlar "balloons". Further zoom-in image of these dendrites can be found in Figure 4.19(B). These dendrites initiated from the electrode surface, and the thick (~700 nm) [PEO-Kevlar]₅₀ prevented them from spreading out on the surface. Perpendicular to the electrode surface was the direction with the least resistance because of the elasticity of PEO-Kevlar membrane. The dendrites went up and differentiated, but the mechanical strength from PEO-Kevlar provided enough surface tension to hold the branched structures together and formed the spheres. Figure 4.19(A) provided direct and strong

evidence that PEO-Kevlar membrane remained intact during the whole deposition process as a thin film connecting the two spheres can clearly be observed (4.19(A), pointed by arrow). No dendrites were able to poke through the PEO-Kevlar membrane throughout the whole process, suggesting a considerable mechanical strength and stability [PEO-Kevlar]₅₀ membrane possessed.

To further confirm and prove the existence of the PEO-Kevlar membrane confining copper dendrites, EDAX with different acceleration voltages was used to probe the PEO-Kevlar-copper laminated structures after dendrite deposition under high deposition current. Zaide and co-workers studied the relationship between acceleration voltages and corresponding penetration depth under SEM imaging:

$$H = \frac{0.0276AE^{1.67}}{(Z^{0.89}D)} \quad (\text{Eq. 4-1})$$

where H is the penetration depth in nanometer, A the atomic weight, E the acceleration voltage in volts, Z the atomic number, and D the density of the material. Table 4.2 lists estimated electron beam penetration depth through PEO-Kevlar-copper laminated structures under acceleration voltage of 2, 5, 10 and 15 kV. Figure 4.20 shows the carbon, oxygen, and copper peaks using EDAX spectroscopy with different acceleration voltages taken on the top of dendrite hemisphere shown in Figure 4.19(B). The sampling area was 100 μm². The ratio between carbon (C) and copper (Cu) under 2 kV of acceleration voltages is significantly higher than that at 15 kV, which gives a very clear indication of the existence of PEO-Kevlar covering the dendrite hemisphere. In Figure 4.21 one can find SEM images of copper dendrites trapped inside PEO-Kevlar membranes. With different acceleration voltages, the penetration depth can be altered. The top three images

were taken with low acceleration voltage, hence the polymer membrane covering the dendrites could be clearly observed. In the bottom three images, high acceleration voltages ranging from 15 to 30 kV were used, and dendrites underneath the PEO-Kevlar membrane could be seen. This is a strong proof that the high mechanical strength of PEO-Kevlar membranes is capable of inhibiting dendrites from shorting the internal circuits of lithium batteries.

With all these experiment results we see very successful dendrite suppression by PEO-Kevlar membranes. PEO-Kevlar system is indeed a very promising system that could potentially solve dendrites issues. One could argue that in the last dendrite suppression experiment demonstrated with long deposition time under lower current density, the spheres formed because there was no pressure on the other side of the membrane, so of course the PEO-Kevlar could freely deform and remain intact. Note that without enough mechanical strength and elasticity, there is not way for a sub-micron polymer thin film to hold off the pressure from metal dendrites growing inside to form a sphere. It's like filling a balloon with water. The balloon needs to have certain strength to reach a certain size. In the experiment we demonstrated that PEO-Kevlar was able to hold off dendrites to the point where more number of atoms were deposited than in an Apple lithium battery, and where the sphere size was comparable to the thickness of commercial separator. Superb mechanical properties of PEO-Kevlar membranes coupled with ionic conductivity represent a big step toward better and more durable lithium metal batteries.

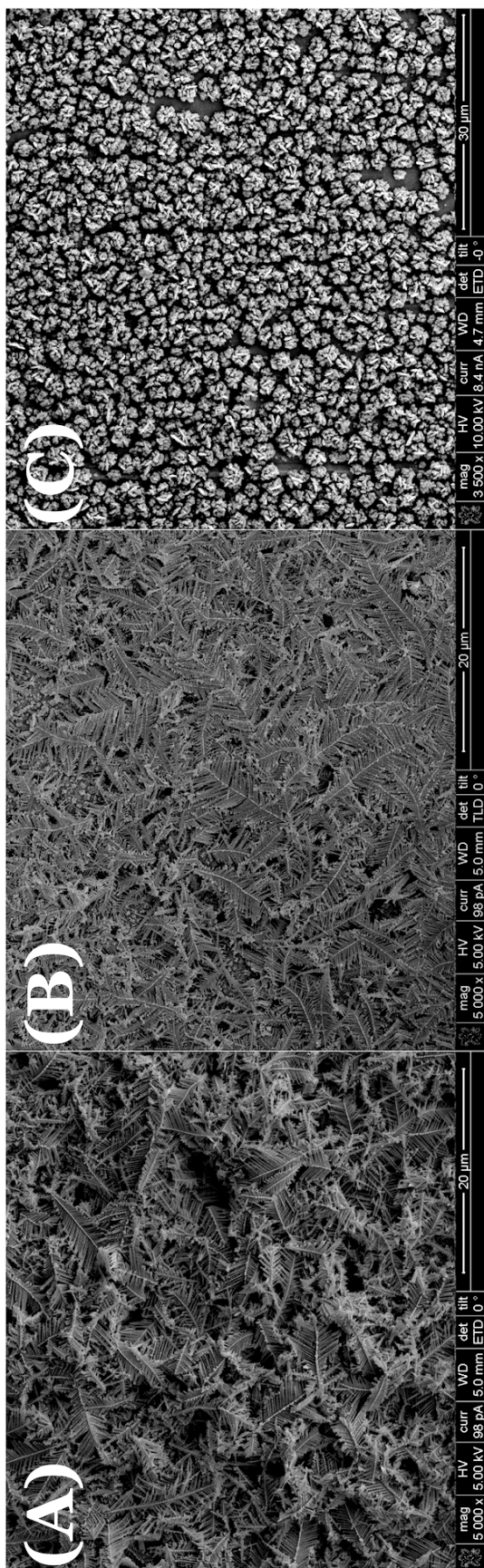


Figure 4.16 Copper dendrite growth with current density of 7.5 mA/cm² on (A) bare copper electrode; (B) copper electrode coated with 10 bilayer of PEO-Kevlar on the surface; and (C) with 20 bilayers of PEO-Kevlar on the surface. Total charge transferred = 2 C (Coulomb).

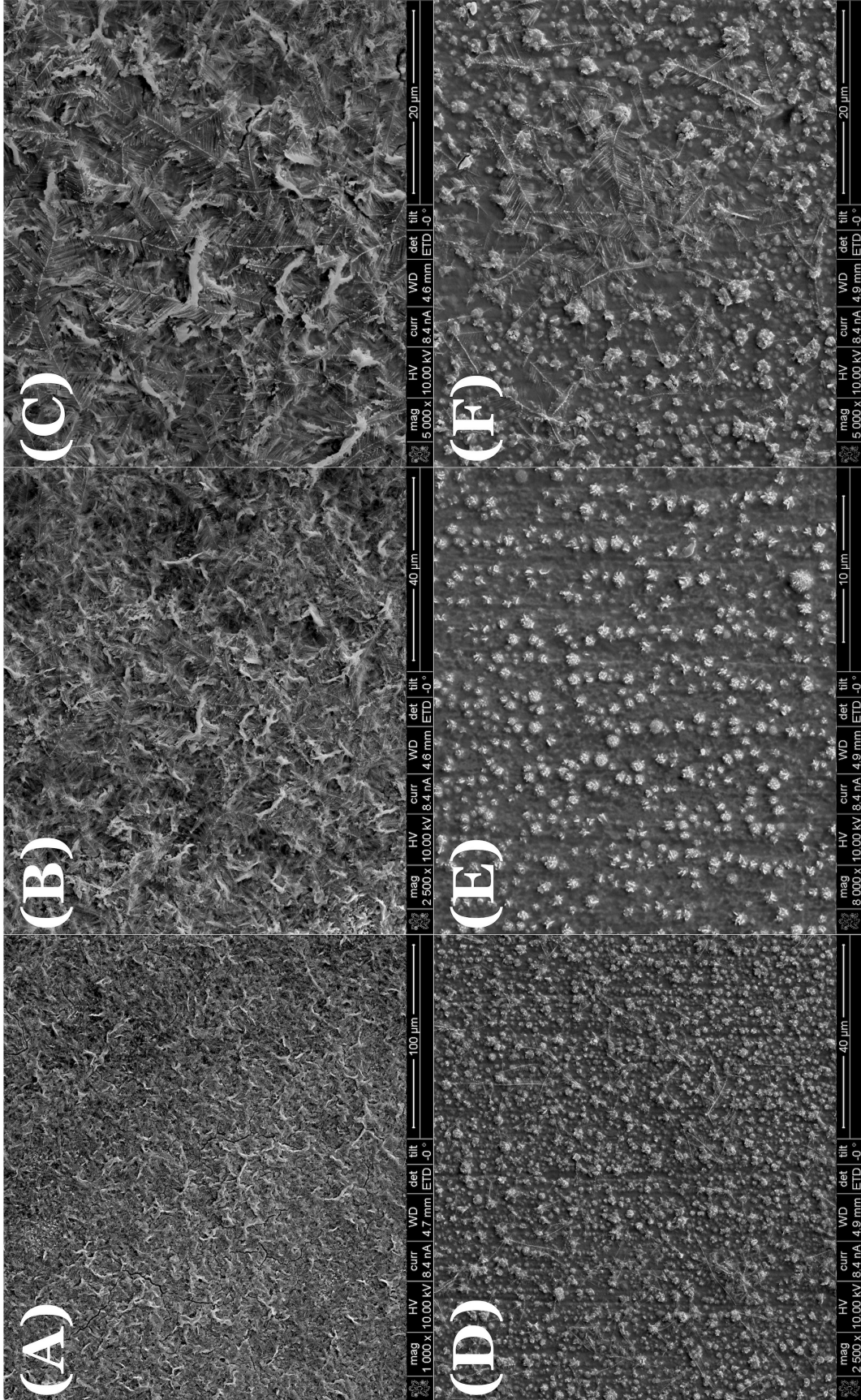


Figure 4.17 Copper dendrite growth under current density of 11.3 mA/cm² on bare copper electrode (A, B, and C) and on copper electrode with 20 bilayers of PEO-Kevlar coating (D, E, and F). Total charge transferred = 0.5 C.

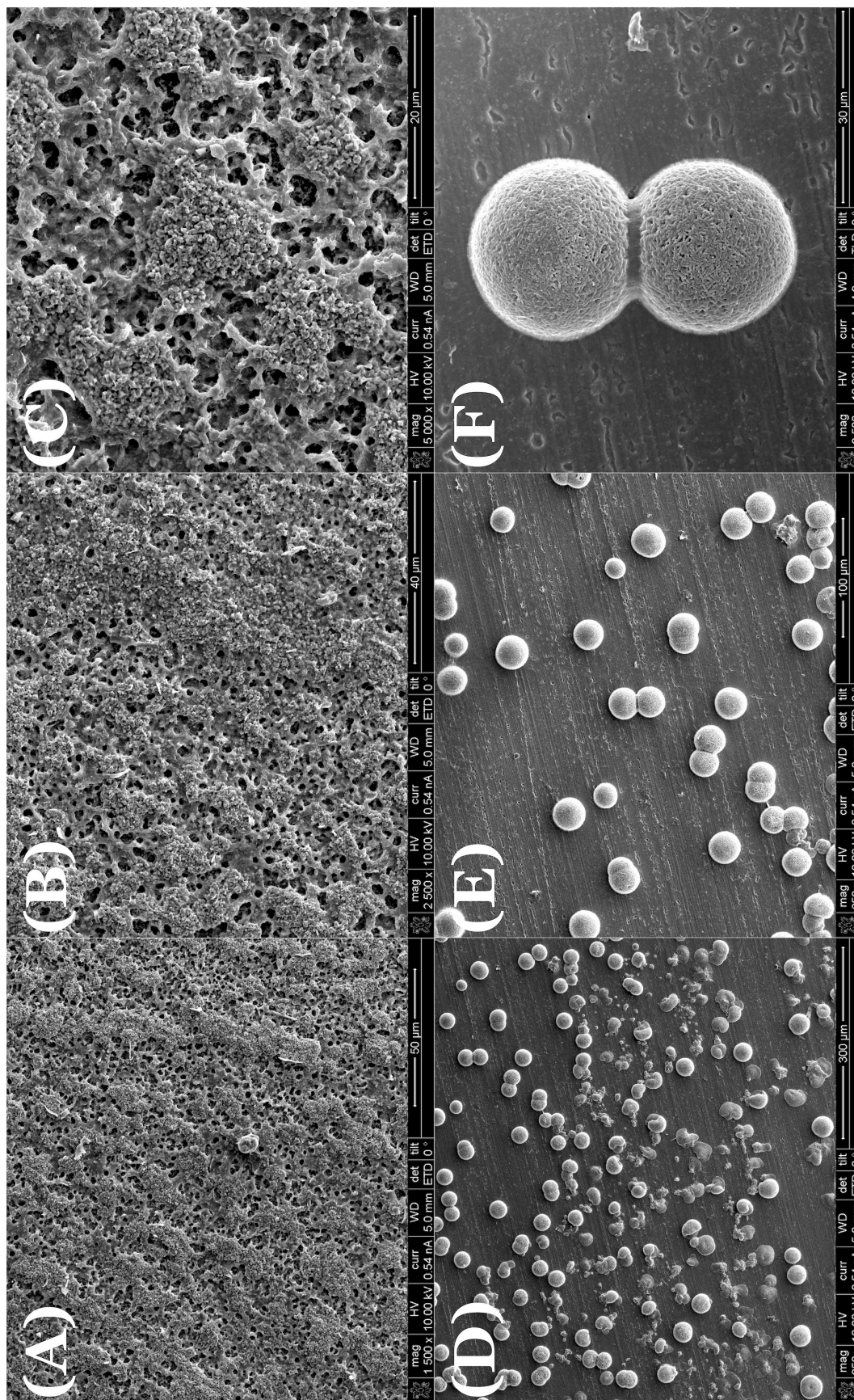


Figure 4.18 Copper dendrite growth under current density of 2.75 mA/cm^2 on bare copper electrode (A, B, and C) and on copper electrode with 50 bilayers of PEO-Kevlar coating (D, E, and F). Total charge transferred = 20 C .

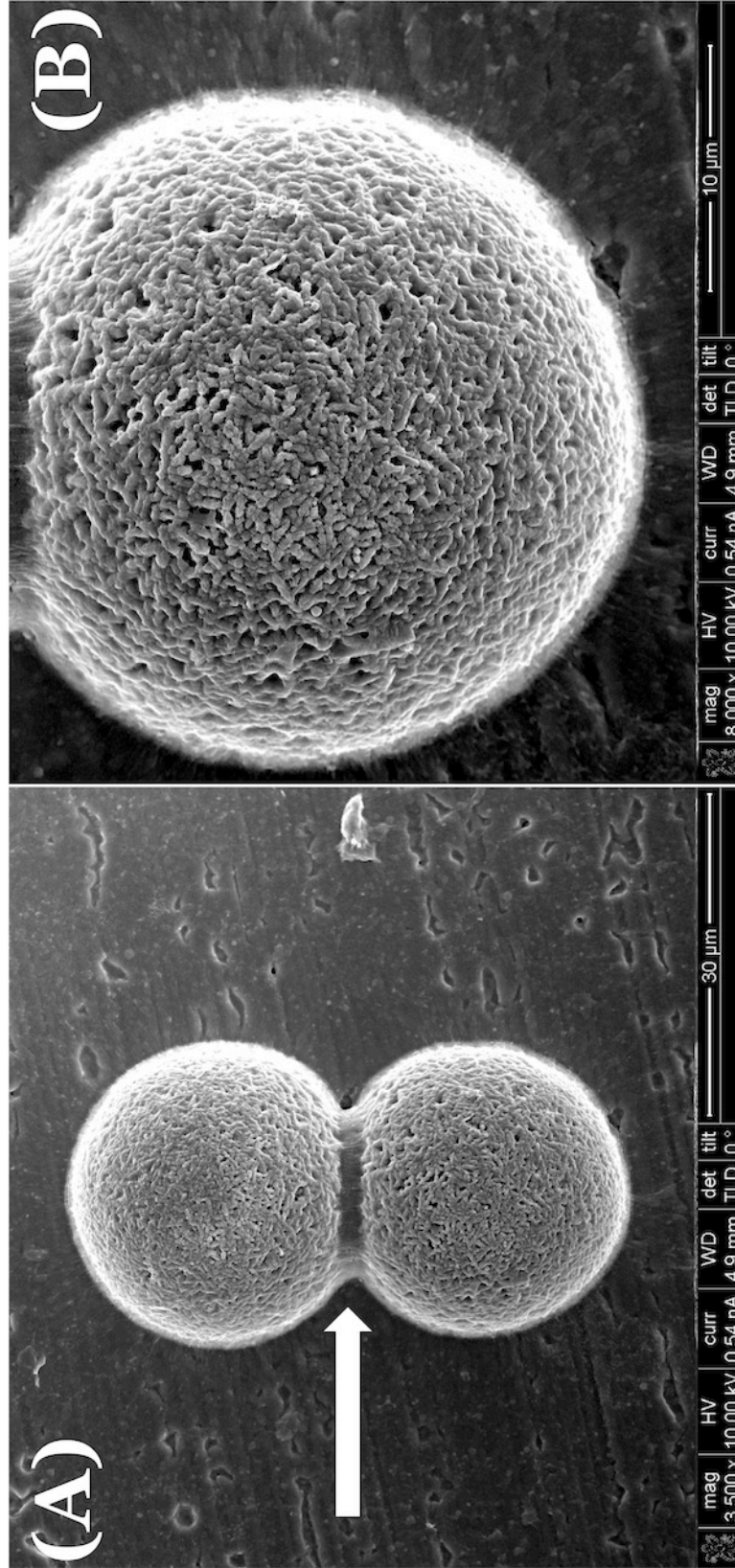


Figure 4.19 Zoomed-in images of Figure 4.X+2(F). PEO-Kevlar membrane is visible in between the two dendrite spheres (indicated by the arrow in (A)) suggesting the wrapping of PEO-Kevlar thin film outside the sphere. Further zoom in, one can see dramatic dendrite structures after vigorous growth being totally confined in the PEO-Kevlar membrane (B).

Voltage (kV)	Penetration (nm)
2	213.78
5	987.48
10	3142.29
15	6184.70

Table 4.2 Estimated electron beam penetration in PEO-Kevlar-copper laminated structures under acceleration voltage of 2, 5, 10, and 15 kV.

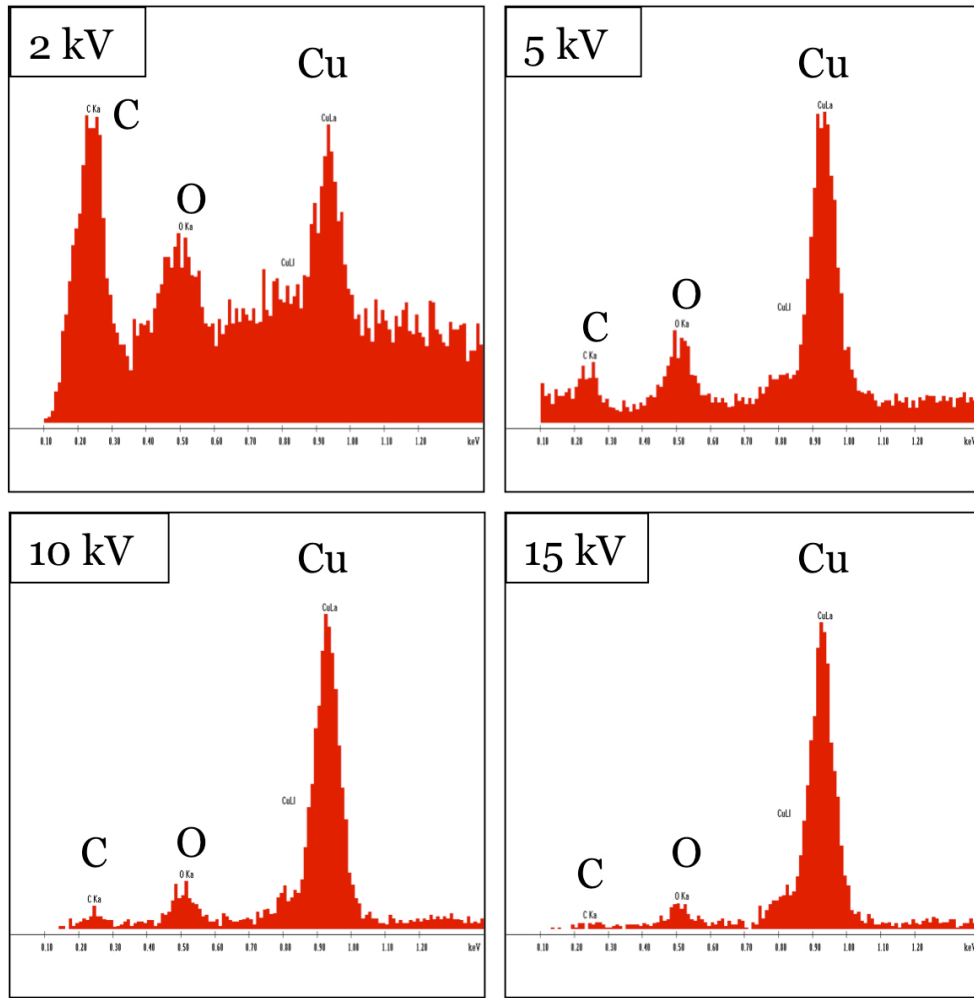


Figure 4.20 EDAX spectroscopy under different acceleration voltages. The ratio between carbon (C) and copper (CU) under different acceleration voltages gives clear indication of the existence of PEO-Kevlar

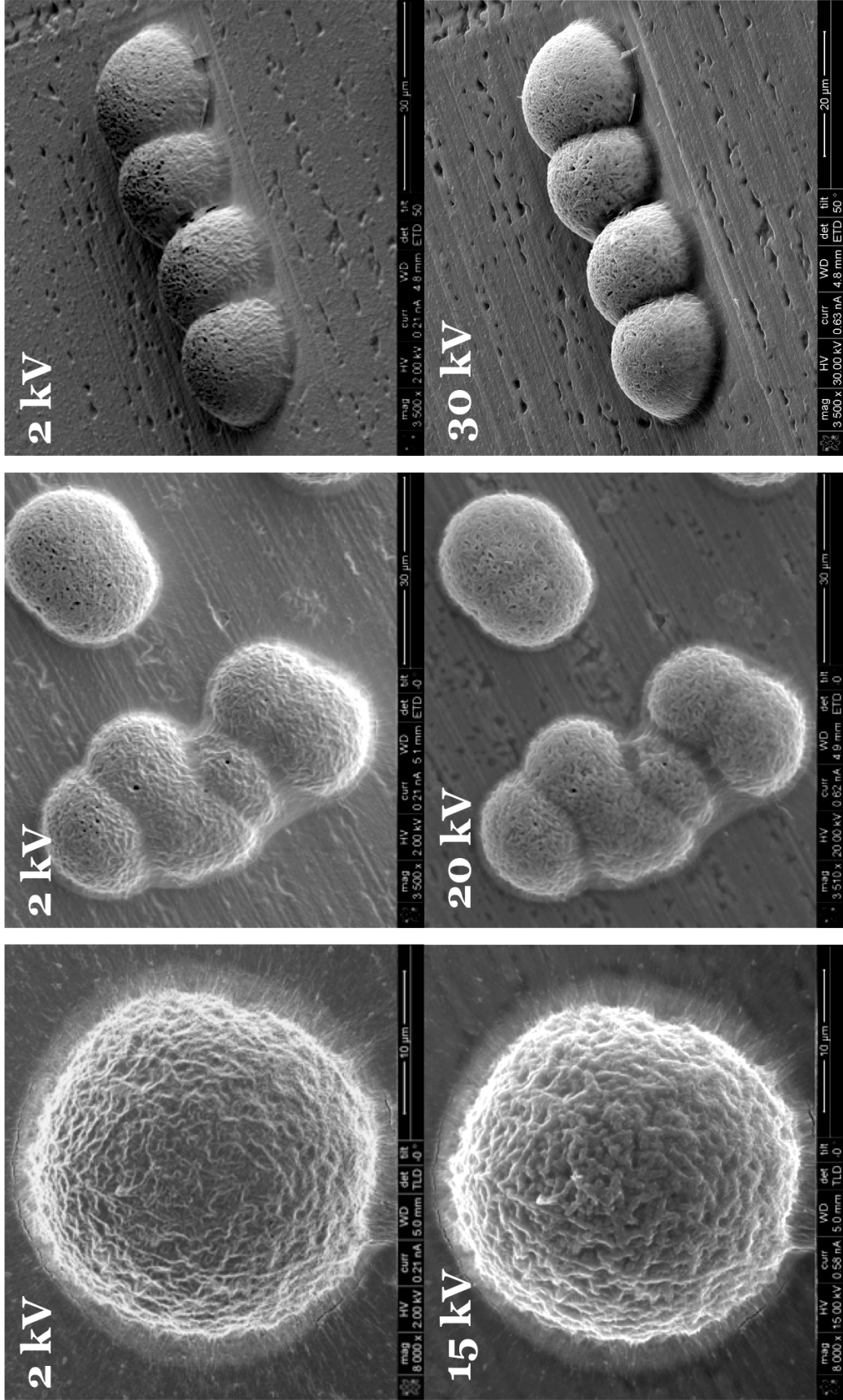


Figure 4.21 SEM images of copper dendrites trapped inside PEO-Kevlar membranes. With different acceleration voltages, the penetration depth can be altered. The top three images were taken with low acceleration voltage, hence the polymer membrane covering the dendrites could be clearly observed. In the bottom three images, high acceleration voltages ranging from 15 to 30 kV were used, and dendrites underneath the PEO-Kevlar membrane could be seen. This is a strong proof that the high mechanical strength of PEO-Kevlar membranes is capable of inhibiting dendrites from shorting the internal circuits of lithium batteries.

4.8 Battery Cell Assembly and Scale-Up

PEO-Kevlar LBL membranes were assembled into half-cells to investigate their functionality. In the half-cell setup, lithium ribbon obtained from Sigma-Aldrich was used as received as anodes. Homemade cathodes consist of lithium manganese oxide, carbon black, and PVDF binder with optimal ratio were made in Argon glovebox. Cathodes were kept inside vacuum oven at 90°C before half-cell assembly to ensure thorough evaporation of NMP solvent. 2032 coin cell casing were used to house half-cell because of their ease of use and availability. PEO-Kelvar membrane with 200 μ l of 1M lithium salt in PC-DMC were sandwiched in between lithium anode and homemade cathode. Figure 4.22(A) shows the cell powering a 5 mW white-light LED successfully. Figure 4.22(B) and (C) demonstrate the ability of scaling up LBL membranes with ease. Basically by substituting the dipping substrates with larger dimensions, one can effortlessly obtain much bigger membrane without any hiccups.

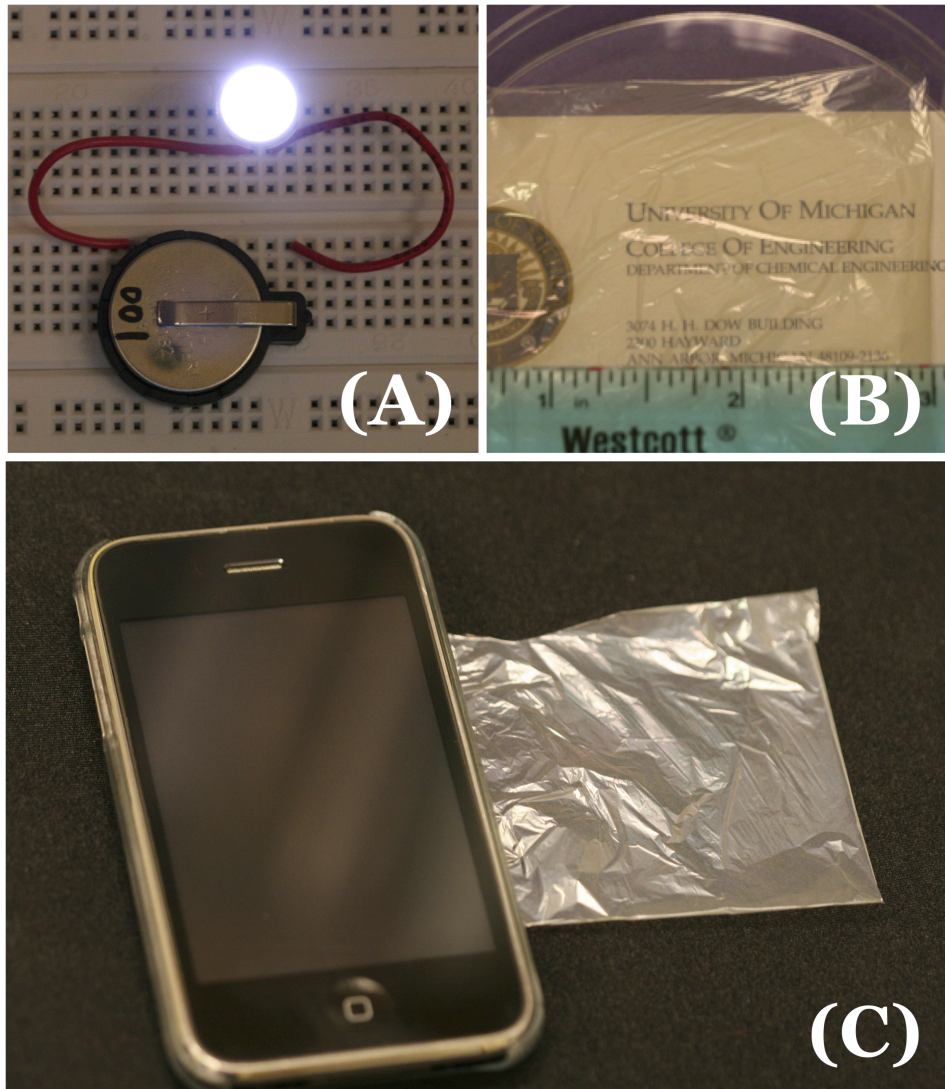


Figure 4.22 (A) PEO-Kevlar ICM in half-cell setup lights up white LED. (B,C) Scaled-up PEO-Kevlar ICM for portable electronic devices.

4.9 Conclusion

In this project we demonstrated a new generation of ionic conducting membrane by combining ionic conducting polymer PEO and the ultrastrong fibrous polymer Kevlar using layer-by-layer assembly. Through layer-by-layer assembly of ionic conducting PEO and robust fibrous polymer Kevlar, the resulting membranes exhibited superior mechanical strength, good conductivity, and high flexibility. With the high flexibility, form-factor will not be an issue when incorporate these state-of-art membrane electrolytes into real-world applications. Electron microscopy showed very uniform surface morphology and cross-section thickness. While crystallization of polymer can degrade performance, XPS results suggested that crystalline structures commonly seen in cast PEO membranes did not exist in LBL membranes. Tensile test results of PEO-Kevlar ICMs indicated superior strength and mechanical modulus that are orders higher than conventional polymer electrolytes. The high mechanical modulus suggests possibility of inhibition of dendrite growth. Electrochemical characterization showed the PEO-Kevlar ICMs possess good ionic conductivity that is high enough for real-world applications. CR 2032 button cell battery incorporated with PEO-Kevlar ICM was shown to power up bright LED.

Chapter 5

Conclusion

In this thesis, we demonstrated and utilized the versatility of layer-by-layer assembly to explore the possibilities of improving membrane characteristics in energy-related applications using such technique. Nanocomposite membranes comprise common polymers and state-of-art nanomaterials were fabricated by LBL technique. Physical, mechanical, optical, and electrochemical properties, as well as performance in actual energy devices were intensively investigated. Carbon nanotube and carbon nanofiber were decorated with Pt nanoparticles and manufactured into freestanding membranes for the use as anodes in fuel cell MEAs and substantially improved performance. Better durability can be expected as LBL membranes are more resistant to harsh environment, although no actual data was collected in this work. Platinum nanoparticles deposited on the sidewalls of SWNT and CF with the incorporation of Nafion could significantly increase the number of catalysis sites and improve the accessibility to tri-phase boundaries (TPBs). Single-walled carbon nanotube (SWNT) and carbon fiber (CF) loading in LBL membranes can be as high as 50% without phase segregation of dissimilar materials. Uniform distribution of nanotubes and nanometer control of the film structure through layer-by-layer assembly contributed to an extensive percolation network, and possibly improved electronic and proton conductivities.

Also, through layer-by-layer assembly, we created thick and uniform coating on ITO electrodes from polyelectrolyte PDDA and negatively charged zeolite-L nanocrystals. SEM images show that most of the deposited disk-shaped zeolite-L nanocrystals are sitting flat on top of each other with the same orientation. Ionic conducting channels inside zeolite-L nanocrystals are hence aligned with c-axis, making the transport in the direction vertical to the electrode surface possible. Electrochemical characterization shows dramatic enhancement of redox peaks when zeolite-L modified electrodes are used, and the thicker the zeolite-L layer, the better the enhancement. By investigating the physiosorption behavior of redox species ferrocyanide in PDDA/zeolite-L LBL composite matrix, we confirm that although ferrocyanide cannot diffuse freely in and out the channel due to the larger size of the channels, the adsorption of ferrocyanide in the PDDA/zeolite-L membranes dramatically increases the concentration of the ferrocyanide molecules in the vicinity of the electrode surface. The active electron/hole conducting nature of zeolite-L nanocrystals also contributes to the increase of active redox surface area. Finally we successfully demonstrate the feasibility of loading PDDA/zeolite-L LBL matrix with foreign molecules, which can turn interesting zeolite-L modified electrodes into molecular probes.

Lastly, a new generation of ionic conducting nanocomposite membranes for lithium batteries was presented. Through layer-by-layer assembly of ionic conducting PEO and robust fibrous polymer Kevlar, the resulting membranes exhibited superior mechanical strength, good conductivity, and high flexibility. Electron microscopy

showed very uniform surface morphology and cross-section thickness. While crystallization of polymer can degrade performance, XPS results suggested that crystalline structures commonly seen in cast PEO membranes did not exist in LBL membranes. Inhibition of re-crystallization of PEO in LBL membranes indicates wider and higher working temperature window. Tensile test results of PEO-Kevlar ICMs indicated superior strength and mechanical modulus that are orders higher than conventional polymer electrolytes. Electrochemical characterization showed the PEO-Kevlar ICMs possess good ionic conductivity that is high enough for real-world applications. CR 2032 button cell battery incorporated with PEO-Kevlar ICM was shown to power up bright LED. Although the mechanical properties of the PEO-Kevlar membranes manufactured in this study did not reach the theoretical values suggested by Monroe *et al*, and more research and development is indeed required, the results from this study represent a step closer to next generation high capacity high power lithium batteries, where dendrites would no longer be an issue, where lithium metal electrodes could be used to optimize and carry out the true potential of lithium batteries.

Bibliography

1. Cui, X.; Chen, W., Saccharin Effects on Direct-Current Electroplating Nanocrystalline Ni–Cu Alloys. *Journal of The Electrochemical Society* **2008**, *155*, K133.
2. Xu, K., Nonaqueous liquid electrolytes for lithium-based rechargeable batteries. *Chemical Reviews* **2004**, *104*, 4303-4418.
3. Leo, C. J.; Thakur, A. K.; Rao, G. V. S.; Chowdari, B. V. R., Effect of glass-ceramic filler on properties of polyethylene oxide-LiCF₃SO₃ complex. *Journal of Power Sources* **2003**, *115* (2), 295-304.
4. Wang, C. S.; Zhang, X. W.; Appleby, A. J., Solvent-free composite PEO-ceramic fiber/mat electrolytes for lithium secondary cells. *Journal of the Electrochemical Society* **2005**, *152* (1), A205-A209.
5. Wu, C. G.; Lu, M. I.; Tsai, C. C.; Chuang, H. J. In *PVdF-HFP/metal oxide nanocomposites: The matrices for high-conducting, low-leakage porous polymer electrolytes*, 3rd International Conference on Materials for Advanced Technologies (ICMAT-2005)/9th International Conference on Advanced Materials (ICAM 2005), Singapore, SINGAPORE, Jul 03-08; Exhibit, C., Ed. Elsevier Science Bv: Singapore, SINGAPORE, 2005; pp 295-300.
6. Osaka, T.; Homma, T.; Momma, T.; Yarimizu, H., In situ observation of lithium deposition processes in solid polymer and gel electrolytes. *Journal of Electroanalytical Chemistry* **1997**, *421* (1-2), 153-156.
7. Hsu, P. C.; Seol, S. K.; Lo, T. N.; Liu, C. J.; Wang, C. L.; Lin, C. S.; Hwu, Y.; Chen, C. H.; Chang, L. W.; Je, J. H.; Margaritondo, G., Hydrogen bubbles and the growth morphology of ramified zinc by electrodeposition. *Journal of the Electrochemical Society* **2008**, *155* (5), D400-D407.
8. Matsushima, H.; Bund, A.; Plieth, W.; Kikuchi, S.; Fukunaka, Y., Copper electrodeposition in a magnetic field. *Electrochimica Acta* **2007**, *53* (1), 161-166.
9. Brissot, C.; Rosso, M.; Chazalviel, J.; Lascaud, S., Dendritic growth mechanisms in lithium/polymer cells. *Journal of Power Sources* **1999**, *81*, 925-929.
10. Despic, A. R. P., K. I., Transport-controlled deposition and dissolution of metals. *Modern Aspects of Electrochemistry* **1972**, *7*, 119.

11. Yamaki, J.; Tobishima, S.; Hayashi, K.; Saito, K.; Nemoto, Y.; Arakawa, M., A consideration of the morphology of electrochemically deposited lithium in an organic electrolyte. *Journal of Power Sources* **1998**, *74* (2), 219-227.
12. Monroe, C.; Newman, J., The impact of elastic deformation on deposition kinetics at lithium/polymer interfaces. *Journal of The Electrochemical Society* **2005**, *152* (2), A396-A404.
13. Gates, B. D.; Xu, Q. B.; Stewart, M.; Ryan, D.; Willson, C. G.; Whitesides, G. M., New approaches to nanofabrication: Molding, printing, and other techniques. *Chemical Reviews* **2005**, *105* (4), 1171-1196.
14. Brus, L. E., Electron Electron and Electron-Hole Interactions in Small Semiconductor Crystallites - the Size Dependence of the Lowest Excited Electronic State. *Journal of Chemical Physics* **1984**, *80* (9), 4403-4409.
15. Feldheim, D. L.; Keating, C. D., Self-assembly of single electron transistors and related devices. *Chemical Society Reviews* **1998**, *27* (1), 1-12.
16. Kastner, M. A., Artificial Atoms. *Physics Today* **1993**, *46* (1), 24-31.
17. Klein, D. L.; Roth, R.; Lim, A. K. L.; Alivisatos, A. P.; McEuen, P. L., A single-electron transistor made from a cadmium selenide nanocrystal. *Nature* **1997**, *389* (6652), 699-701.
18. Ho, S. S.; Critchley, K.; Lilly, G. D.; Shim, B.; Kotov, N. A., Free flow electrophoresis for the separation of CdTe nanoparticles. *Journal of Materials Chemistry* **2009**, *19* (10), 1390-1394.
19. Lee, J.; Hernandez, P.; Lee, J.; Govorov, A. O.; Kotov, N. A., Exciton-plasmon interactions in molecular spring assemblies of nanowires and wavelength-based protein detection. *Nature Materials* **2007**, *6* (4), 291-295.
20. Tang, Z. Y.; Zhang, Z. L.; Wang, Y.; Glotzer, S. C.; Kotov, N. A., Self-assembly of CdTe nanocrystals into free-floating sheets. *Science* **2006**, *314* (5797), 274-278.
21. Tang, Z. Y.; Kotov, N. A., One-dimensional assemblies of nanoparticles: Preparation, properties, and promise. *Advanced Materials* **2005**, *17* (8), 951-962.
22. Lee, J.; Govorov, A. O.; Dulka, J.; Kotov, N. A., Bioconjugates of CdTe nanowires and Au nanoparticles: Plasmon-exciton interactions, luminescence enhancement, and collective effects. *Nano Letters* **2004**, *4* (12), 2323-2330.
23. Tang, Z. Y.; Kotov, N. A.; Giersig, M., Spontaneous organization of single CdTe nanoparticles into luminescent nanowires. *Science* **2002**, *297* (5579), 237-240.

24. Venema, L. C.; Wildoer, J. W. G.; Janssen, J. W.; Tans, S. J.; Tuinstra, H. L. J. T.; Kouwenhoven, L. P.; Dekker, C., Imaging electron wave functions of quantized energy levels in carbon nanotubes. *Science* **1999**, *283* (5398), 52-55.
25. Avouris, P.; Martel, R.; Derycke, V.; Appenzeller, J., Carbon nanotube transistors and logic circuits. *Physica B-Condensed Matter* **2002**, *323* (1-4), 6-14.
26. Zhou, C. W.; Kong, J.; Yenilmez, E.; Dai, H. J., Modulated chemical doping of individual carbon nanotubes. *Science* **2000**, *290* (5496), 1552-1555.
27. Liang, W. J.; Bockrath, M.; Bozovic, D.; Hafner, J. H.; Tinkham, M.; Park, H., Fabry-Perot interference in a nanotube electron waveguide. *Nature* **2001**, *411* (6838), 665-669.
28. Bockrath, M.; Liang, W. J.; Bozovic, D.; Hafner, J. H.; Lieber, C. M.; Tinkham, M.; Park, H. K., Resonant electron scattering by defects in single-walled carbon nanotubes. *Science* **2001**, *291* (5502), 283-285.
29. Bockrath, M.; Cobden, D. H.; McEuen, P. L.; Chopra, N. G.; Zettl, A.; Thess, A.; Smalley, R. E., Single-electron transport in ropes of carbon nanotubes. *Science* **1997**, *275* (5308), 1922-1925.
30. Baughman, R. H.; Cui, C. X.; Zakhidov, A. A.; Iqbal, Z.; Barisci, J. N.; Spinks, G. M.; Wallace, G. G.; Mazzoldi, A.; De Rossi, D.; Rinzler, A. G.; Jaschinski, O.; Roth, S.; Kertesz, M., Carbon nanotube actuators. *Science* **1999**, *284* (5418), 1340-1344.
31. Colburn, M.; Johnson, S.; Stewart, M.; Damle, S.; Bailey, T.; Choi, B.; Wedlake, M.; Michaelson, T.; Sreenivasan, S. V.; Ekerdt, J.; Willson, C. G., Step and flash imprint lithography: A new approach to high-resolution patterning. *Emerging Lithographic Technologies Iii, Pts 1 and 2* **1999**, *3676*, 379-389
864.
32. Xia, Y. N.; Kim, E.; Zhao, X. M.; Rogers, J. A.; Prentiss, M.; Whitesides, G. M., Complex optical surfaces formed by replica molding against elastomeric masters. *Science* **1996**, *273* (5273), 347-349.
33. Chou, S. Y.; Krauss, P. R.; Renstrom, P. J., Imprint lithography with 25-nanometer resolution. *Science* **1996**, *272* (5258), 85-87.
34. Xia, Y. N.; Whitesides, G. M., Soft lithography. *Annual Review of Materials Science* **1998**, *28*, 153-184.
35. Xia, Y. A.; Venkateswaran, N.; Qin, D.; Tien, J.; Whitesides, G. M., Use of electroless silver as the substrate in microcontact printing of alkanethiols and its application in microfabrication. *Langmuir* **1998**, *14* (2), 363-371.

36. Whitesides, G. M.; Mathias, J. P.; Seto, C. T., Molecular Self-Assembly and Nanochemistry - a Chemical Strategy for the Synthesis of Nanostructures. *Science* **1991**, 254 (5036), 1312-1319.
37. Boncheva, M.; Bruzewicz, D. A.; Whitesides, G. M., Millimeter-scale self-assembly and its applications. *Pure and Applied Chemistry* **2003**, 75 (5), 621-630.
38. Glotzer, S. C.; Solomon, M. J.; Kotov, N. A., Self-assembly: From nanoscale to microscale colloids. *Aiche Journal* **2004**, 50 (12), 2978-2985.
39. Kotov, N. A.; Haraszti, T.; Turi, L.; Zavala, G.; Geer, R. E.; Dekany, I.; Fendler, J. H., Mechanism of and defect formation in the self-assembly of polymeric polycation-montmorillonite ultrathin films. *Journal of the American Chemical Society* **1997**, 119 (29), 6821-6832.
40. Kotov, N. A.; Dekany, I.; Fendler, J. H., Ultrathin graphite oxide-polyelectrolyte composites prepared by self-assembly: Transition between conductive and non-conductive states. *Advanced Materials* **1996**, 8 (8), 637-&.
41. Fuchs, H.; Ohst, H.; Prass, W., Ultrathin Organic Films - Molecular Architectures for Advanced Optical, Electronic and Bio-Related Systems. *Advanced Materials* **1991**, 3 (1), 10-18.
42. Decher, G.; Hong, J. D.; Lowack, K.; Lvov, Y.; Schmitt, J., Layer-by-Layer Adsorption - the Solid Liquid-Interface as a Template for the Controlled Growth of Well-Defined Nanostructures of Polyelectrolytes, Proteins, DNA and Polynucleotides. *Self-Production of Supramolecular Structures* **1994**, 446, 267-272.
43. Lvov, Y.; Decher, G.; Mohwald, H., Assembly, Structural Characterization, and Thermal-Behavior of Layer-by-Layer Deposited Ultrathin Films of Poly(Vinyl Sulfate) and Poly(Allylamine). *Langmuir* **1993**, 9 (2), 481-486.
44. Decher, G., Fuzzy nanoassemblies: Toward layered polymeric multicomposites. *Science* **1997**, 277 (5330), 1232-1237.
45. Ferreira, M.; Rubner, M. F., Molecular-Level Processing of Conjugated Polymers .1. Layer-by-Layer Manipulation of Conjugated Polyions. *Macromolecules* **1995**, 28 (21), 7107-7114.
46. Fou, A. C.; Rubner, M. F., Molecular-Level Processing of Conjugated Polymers .2. Layer-by-Layer Manipulation of in-Situ Polymerized P-Type Doped Conducting Polymers. *Macromolecules* **1995**, 28 (21), 7115-7120.
47. Cheung, J. H.; Stockton, W. B.; Rubner, M. F., Molecular-level processing of conjugated polymers .3. Layer-by-layer manipulation of polyaniline via electrostatic interactions. *Macromolecules* **1997**, 30 (9), 2712-2716.

48. Stockton, W. B.; Rubner, M. F., Molecular-level processing of conjugated polymers .4. Layer-by-layer manipulation of polyaniline via hydrogen-bonding interactions. *Macromolecules* **1997**, *30* (9), 2717-2725.
49. Kotov, N. A., Layer-by-layer self-assembly: The contribution of hydrophobic interactions. *Nanostructured Materials* **1999**, *12* (5-8), 789-796.
50. Kotov, N. A.; Magonov, S.; Tropsha, E., Layer-by-layer self-assembly of aluminosilicate-polyelectrolyte composites: Mechanism of deposition, crack resistance, and perspectives for novel membrane materials. *Chemistry of Materials* **1998**, *10* (3), 886-895.
51. Kotov, N. A.; Dekany, I.; Fendler, J. H., Layer-by-Layer Self-Assembly of Polyelectrolyte-Semiconductor Nanoparticle Composite Films. *Journal of Physical Chemistry* **1995**, *99* (35), 13065-13069.
52. Srivastava, S.; Kotov, N. A., Composite Layer-by-Layer (LBL) Assembly with Inorganic Nanoparticles and Nanowires. *Accounts of Chemical Research* **2008**, *41* (12), 1831-1841.
53. Kotov, N. A., Layer-by-layer assembled films of nanoparticles: Materials perspectives and photonics and biophotonics applications. *Leos 2001: 14th Annual Meeting of the Ieee Lasers & Electro-Optics Society, Vols 1 and 2, Proceedings* **2001**, 388-389
907.
54. Liz-Marzan, L. M.; Pastoriza-Santos, I.; Kotov, N. A.; Malikova, N., Layer-by-layer assembled planar gold nanoparticles. *Abstracts of Papers of the American Chemical Society* **2002**, *224*, U331-U331.
55. Malikova, N.; Pastoriza-Santos, I.; Schierhorn, M.; Kotov, N. A.; Liz-Marzan, L. M., Layer-by-layer assembled mixed spherical and planar gold nanoparticles: Control of interparticle interactions. *Langmuir* **2002**, *18* (9), 3694-3697.
56. Mamedov, A. A.; Kotov, N. A., Free-standing layer-by-layer assembled films of magnetite nanoparticles. *Langmuir* **2000**, *16* (13), 5530-5533.
57. Rogach, A. L.; Koktysh, D. S.; Harrison, M.; Kotov, N. A., Layer-by-layer assembled films of HgTe nanocrystals with strong infrared emission. *Chemistry of Materials* **2000**, *12* (6), 1526-+.
58. Srivastava, S.; Podsiadlo, P.; Critchley, K.; Zhu, J.; Qin, M.; Shim, B. S.; Kotov, N. A., Single-Walled Carbon Nanotubes Spontaneous Loading into Exponentially Grown LBL Films. *Chemistry of Materials* **2009**, *21* (19), 4397-4400.
59. Shim, B. S.; Tang, Z. Y.; Morabito, M. P.; Agarwal, A.; Hong, H. P.; Kotov, N. A., Integration of conductivity transparency, and mechanical strength into highly

- homogeneous layer-by-layer composites of single-walled carbon nanotubes for optoelectronics. *Chemistry of Materials* **2007**, *19* (23), 5467-5474.
60. Shim, B. S.; Kotov, N. A., Single-walled carbon nanotube combing during layer-by-layer assembly: From random adsorption to aligned composites. *Langmuir* **2005**, *21* (21), 9381-9385.
61. Wang, Y.; Tang, Z. Y.; Podsiadlo, P.; Elkasabi, Y.; Lahann, J.; Kotov, N. A., Mirror-like photoconductive layer-by-layer thin films of Te nanowires: The fusion of semiconductor, metal, and insulator properties. *Advanced Materials* **2006**, *18* (4), 518-+.
62. Podsiadlo, P.; Shim, B. S.; Kotov, N. A., Polymer/clay and polymer/carbon nanotube hybrid organic-inorganic multilayered composites made by sequential layering of nanometer scale films. *Coordination Chemistry Reviews* **2009**, *253* (23-24), 2835-2851.
63. Podsiadlo, P.; Paternel, S.; Rouillard, J. M.; Zhang, Z. F.; Lee, J.; Lee, J. W.; Gulari, L.; Kotov, N. A., Layer-by-layer assembly of nacre-like nanostructured composites with antimicrobial properties. *Langmuir* **2005**, *21* (25), 11915-11921.
64. Podsiadlo, P.; Liu, Z. Q.; Paterson, D.; Messersmith, P. B.; Kotov, N. A., Fusion of seashell nacre and marine bioadhesive analogs: High-strength nanocomposite by layer-by-layer assembly of clay and L-3,4-dihydroxyphenylalanine polymer. *Advanced Materials* **2007**, *19* (7), 949-+.
65. Mehta, G.; Kiel, M. J.; Lee, J. W.; Kotov, N.; Linderman, J. J.; Takayama, S., Polyelectrolyte-clay-protein layer films on microfluidic PDMS bioreactor surfaces for primary murine bone marrow culture. *Advanced Functional Materials* **2007**, *17* (15), 2701-2709.
66. Tang, Z. Y.; Wang, Y.; Podsiadlo, P.; Kotov, N. A., Biomedical applications of layer-by-layer assembly: From biomimetics to tissue engineering. *Advanced Materials* **2006**, *18* (24), 3203-3224.
67. Wong, S. Y.; Li, Q.; Veselinovic, J.; Kim, B. S.; Klibanov, A. M.; Hammond, P. T., Bactericidal and virucidal ultrathin films assembled layer by layer from polycationic N-alkylated polyethylenimines and polyanions. *Biomaterials* **2010**, *31* (14), 4079-4087.
68. Barros, E. B.; Jorio, A.; Samsonidze, G. G.; Capaz, R. B.; Souza, A. G.; Mendes, J.; Dresselhaus, G.; Dresselhaus, M. S., Review on the symmetry-related properties of carbon nanotubes. *Physics Reports-Review Section of Physics Letters* **2006**, *431* (6), 261-302.
69. Jessel, N.; Atalar, F.; Lavalle, P.; Mutterer, J.; Decher, G.; Schaaf, P.; Voegel, J. C.; Ogier, J., Bioactive coatings based on a polyelectrolyte multilayer architecture functionalized by embedded proteins. *Advanced Materials* **2003**, *15* (9), 692-695.

70. Mamedov, A. A.; Kotov, N. A., Layer-by-layer assembled gradient CdTe/polymer films. *Abstracts of Papers of the American Chemical Society* **2001**, *221*, U351-U351.
71. Ostrander, J. W.; Mamedov, A. A.; Kotov, N. A., Two modes of linear layer-by-layer growth of nanoparticle-polyelectrolyte multilayers and different interactions in the layer-by-layer deposition. *Journal of the American Chemical Society* **2001**, *123* (6), 1101-1110.
72. Tang, Z. Y.; Kotov, N. A.; Magonov, S.; Ozturk, B., Nanostructured artificial nacre. *Nature Materials* **2003**, *2* (6), 413-U8.
73. Rouse, J. H.; Ounales, Z.; T Lellehei, P. T.; Siochi, E. J., Incorporation of carbon nanotubes within stepwise assembled polyelectrolyte films. *Abstracts of Papers of the American Chemical Society* **2002**, *223*, U398-U398.
74. Fu, Y.; Bai, S. L.; Cui, S. X.; Qiu, D. L.; Wang, Z. Q.; Zhang, X., Hydrogen-bonding-directed layer-by-layer multilayer assembly: Reformation yielding microporous films. *Macromolecules* **2002**, *35* (25), 9451-9458.
75. Cruz, F. J. A. L.; Muller, E. A., Behavior of ethylene and ethane within single-walled carbon nanotubes. 1-Adsorption and equilibrium properties. *Adsorption-Journal of the International Adsorption Society* **2009**, *15* (1), 1-12.
76. Pan, M.; Tang, H. L.; Jiang, S. P.; Liu, Z. C., Fabrication and performance of polymer electrolyte fuel cells by self-assembly of Pt nanoparticles. *Journal of the Electrochemical Society* **2005**, *152* (6), A1081-A1088.
77. Farhat, T. R.; Hammond, P. T., Designing a new generation of proton-exchange membranes using layer-by-layer deposition of polyelectrolytes. *Advanced Functional Materials* **2005**, *15* (6), 945-954.
78. Jiang, S. P.; Liu, Z. C.; Tian, Z. Q., Layer-by-layer self-assembly of composite polyelectrolyte-nafion membranes for direct methanol fuel cells. *Advanced Materials* **2006**, *18* (8), 1068-+.
79. Farhat, T. R.; Hammond, P. T., Fabrication of a "soft" membrane electrode assembly using layer-by-layer technology. *Advanced Functional Materials* **2006**, *16* (3), 433-444.
80. Farhat, T. R.; Hammond, P. T., Engineering ionic and electronic conductivity in polymer catalytic electrodes using the layer-by-layer technique. *Chemistry of Materials* **2006**, *18* (1), 41-49.
81. Kostelansky, C. N.; Pietron, J. J.; Chen, M. S.; Dressick, W. J.; Swider-Lyons, K. E.; Ramaker, D. E.; Stroud, R. M.; Klug, C. A.; Zelakiewicz, B. S.; Schull, T. L., Triarylphosphine-stabilized platinum nanoparticles in three-dimensional nanostructured films as active electrocatalysts. *Journal of Physical Chemistry B* **2006**, *110* (43), 21487-21496.

82. Choi, K. H.; Kim, H. S.; Lee, T. H., Electrode fabrication for proton exchange membrane fuel cells by pulse electrodeposition. *Journal of Power Sources* **1998**, *75* (2), 230-235.
83. Antoine, O.; Durand, R., In situ electrochemical deposition of Pt nanoparticles on carbon and inside Nafion. *Electrochemical and Solid State Letters* **2001**, *4* (5), A55-A58.
84. Kim, H.; Popov, B. N., Development of novel method for preparation of PEMFC electrodes. *Electrochemical and Solid State Letters* **2004**, *7* (4), A71-A74.
85. Hirano, S.; Kim, J.; Srinivasan, S., High performance proton exchange membrane fuel cells with sputter-deposited Pt layer electrodes. *Electrochimica Acta* **1997**, *42* (10), 1587-1593.
86. Witham, C. K.; Chun, W.; Valdez, T. I.; Narayanan, S. R., Performance of direct methanol fuel cells with sputter-deposited anode catalyst layers. *Electrochemical and Solid State Letters* **2000**, *3* (11), 497-500.
87. Cha, S. Y.; Lee, W. M., Performance of proton exchange membrane fuel cell electrodes prepared by direct deposition of ultrathin platinum on the membrane surface. *Journal of the Electrochemical Society* **1999**, *146* (11), 4055-4060.
88. Haug, A. T.; White, R. E.; Weidner, J. W.; Huang, W.; Shi, S.; Stoner, T.; Rana, N., Increasing proton exchange membrane fuel cell catalyst effectiveness through sputter deposition. *Journal of the Electrochemical Society* **2002**, *149* (3), A280-A287.
89. Lefebvre, M. C.; Qi, Z. G.; Pickup, P. G., Electronically conducting proton exchange polymers as catalyst supports for proton exchange membrane fuel cells - Electrocatalysis of oxygen reduction, hydrogen oxidation, and methanol oxidation. *Journal of the Electrochemical Society* **1999**, *146* (6), 2054-2058.
90. Wang, Y.; Xu, X.; Tian, Z. Q.; Zong, Y.; Cheng, H. M.; Lin, C. J., Selective heterogeneous nucleation and growth of size-controlled metal nanoparticles on carbon nanotubes in solution. *Chemistry-a European Journal* **2006**, *12* (9), 2542-2549.
91. Michel, M.; Taylor, A.; Sekol, R.; Podsiadlo, P.; Ho, P.; Kotov, N.; Thompson, L., High-performance nanostructured membrane electrode, assemblies for fuel cells made by layer-by-layer assembly of carbon nanocolloids. *Advanced Materials* **2007**, *19* (22), 3859-+.
92. Murray, R. W., Frontiers in Electroanalytical Chemistry. *Analytical Chemistry* **1994**, *66* (23), A1162-A1162.
93. Murray, R. W., Nanoelectrochemistry: Metal nanoparticles, nanoelectrodes, and nanopores. *Chemical Reviews* **2008**, *108* (7), 2688-2720.
94. Murray, R. W.; Mcdevitt, J. T.; Longmire, M.; Gollmar, R.; Jernigan, J. C.; Dalton, E. F.; Mccarley, R.; Little, W. A.; Lee, G. T.; Holcomb, M. J.; Hutchinson, J. E.;

- Collman, J. P., Electrochemistry at Yba₂cu₃o₇ Superconductor Electrodes at Temperatures above T_c. *Abstracts of Papers of the American Chemical Society* **1988**, 196, 19-ANYL.
95. Murray, R. W.; Ewing, A. G.; Durst, R. A., Chemically Modified Electrodes - Molecular Design for Electroanalysis. *Analytical Chemistry* **1987**, 59 (5), A379-&.
96. Murray, R. W., Chemically Modified Electrodes. *Electroanalytical Chemistry* **1984**, 13, 191-368.
97. Murray, R. W., Chemically Modified Electrodes for Electrocatalysis. *Philosophical Transactions of the Royal Society of London Series a-Mathematical Physical and Engineering Sciences* **1981**, 302 (1468), 253-265.
98. Murray, R. W., Chemically Modified Electrodes. *Accounts of Chemical Research* **1980**, 13 (5), 135-141.
99. Arvand, M.; Kermanian, M.; Zanjanchi, M. A., Direct determination of aluminium in foods and pharmaceutical preparations by potentiometry using an AIMCM-41 modified polymeric membrane sensor. *Electrochimica Acta* **2010**, 55 (23), 6946-6952.
100. Babaei, A.; Khalilzadeh, B.; Afrasiabi, M., A new sensor for the simultaneous determination of paracetamol and mefenamic acid in a pharmaceutical preparation and biological samples using copper(II) doped zeolite modified carbon paste electrode. *Journal of Applied Electrochemistry* **2010**, 40 (8), 1537-1543.
101. Gligor, D.; Maicaneanu, A.; Walcarius, A., Iron-enriched natural zeolite modified carbon paste electrode for H₂O₂ detection. *Electrochimica Acta* **2010**, 55 (12), 4050-4056.
102. Senthilkumar, S.; Saraswathi, R., Electrochemical sensing of cadmium and lead ions at zeolite-modified electrodes: Optimization and field measurements. *Sensors and Actuators B-Chemical* **2009**, 141 (1), 65-75.
103. Pop, A.; Manea, F.; Radovan, C.; Malchev, P.; Bebeselea, A.; Proca, C.; Burtica, G.; Picken, S.; Schoonman, J., Amperometric Detection of 4-Chlorophenol on Two Types of Expanded Graphite Based Composite Electrodes. *Electroanalysis* **2008**, 20 (22), 2460-2466.
104. Ouf, A. M. A.; Elhafeez, A. M. A.; El-Shafei, A. A., Ethanol oxidation at metal-zeolite-modified electrodes in alkaline medium. Part-1: gold-zeolite-modified graphite electrode. *Journal of Solid State Electrochemistry* **2008**, 12 (5), 601-607.
105. Mbouguen, J. K.; Ngameni, E.; Walcarius, A., Organoclay-enzyme film electrodes. *Analytica Chimica Acta* **2006**, 578 (2), 145-155.
106. Liou, Y. W.; Wang, C. M., Fe(phen)₃(²⁺)-modified zeolite particles and their energetic studies. *Journal of the Chinese Chemical Society* **2002**, 49 (1), 51-56.

107. Walcarius, A.; Devoy, J.; Bessiere, J., Silica-modified electrode for the selective detection of mercury. *Journal of Solid State Electrochemistry* **2000**, 4 (6), 330-336.
108. Walcarius, A.; Luthi, N.; Blin, J. L.; Su, B. L.; Lamberts, L., Electrochemical evaluation of polysiloxane-immobilized amine ligands for the accumulation of copper(II) species. *Electrochimica Acta* **1999**, 44 (25), 4601-4610.
109. Walcarius, A., Zeolite-modified electrodes in electroanalytical chemistry. *Analytica Chimica Acta* **1999**, 384 (1), 1-16.
110. Alvaro, M.; Cabeza, J. F.; Corma, A.; Garcia, H.; Peris, E., Electrochemiluminescence of zeolite-encapsulated poly(p-phenylenevinylene). In *Journal of the American Chemical Society*, 2007; Vol. 129, pp 8074-+.
111. Calzaferri, G.; Lutkouskaya, K., Mimicking the antenna system of green plants. In *Photoch Photobio Sci*, 2008; Vol. 7, pp 879-910.
112. King, S. T., Reaction Mechanism of Oxidative Carbonylation of Methanol to Dimethyl Carbonate in Cu–Y Zeolite. *Journal of Catalysis* **1996**.
113. Lee; Ha, K.; Jung, C.; Lee, Y. J.; Chun, Y. S.; Kim, D.; Rhee ..., B. K., Aligned inclusion of hemicyanine dyes into silica zeolite films for second harmonic generation. *Journal of the American Chemical Society* **2004**.
114. Sun, T.; Seff, K., Silver Clusters and Chemistry in Zeolites. *Chemical Reviews* **1994**.
115. Tajima, K.; Aida, T., Controlled polymerizations with constrained geometries. In *Chemical Communications*, 2000; pp 2399-2412.
116. Tsotsalas, M.; Busby, M.; Gianolio, E.; Aime, S.; De Cola, L., Functionalized nanocontainers as dual magnetic and optical probes for molecular imaging applications. In *CHEMISTRY OF MATERIALS*, 2008; Vol. 20, pp 5888-5893.
117. Calzaferri, G.; Huber, S.; Maas, H.; Minkowski, C., Host-guest antenna materials. In *Angewandte Chemie-International Edition*, 2003; Vol. 42, pp 3732-3758.
118. Popovic, Z.; Otter, M.; Calzaferri, G.; De Cola, L., Selbstorganisation lebender Systeme mit funktionalen Nanomaterialien. *ANGEWANDTE CHEMIE* **2007**.
119. Popovic; Busby, M.; Huber, S.; Calzaferri, G.; De Cola, L., Assembling micro crystals through cooperative coordinative interactions. *Angew Chem Int Ed Engl* **2007**.
120. Anderson, P. A.; Armstrong, A. R.; Edwards, P. P., IONISIERUNG UND EKELTRONENDEKOKALISIERUNG IN KALIUM-ZEOLITH-L: EINE KOMBINIERT NEUTRONENBEUGUNGS- *ANGEWANDTE CHEMIE* **1994**.

121. Minkowski, C.; Pansu, R.; Takano, M.; Calzaferri, G., Energy collection, transport, and trapping by a supramolecular organization of dyes in hexagonal *Advanced Functional Materials* **2006**.
122. Bowden, N. B.; Weck, M.; Choi, I. S.; Whitesides, G. M., Molecule-mimetic chemistry and mesoscale self-assembly. In *Accounts Chem Res*, 2001; Vol. 34, pp 231-238.
123. Kulak, A.; Lee, Y. J.; Park, Y. S.; Yoon, K. B., Orientation-controlled monolayer assembly of zeolite crystals on glass and mica by covalent linkage of surface-bound epoxide and amine groups. In *Angewandte Chemie-International Edition*, 2000; Vol. 39, pp 950-+.
124. Kulak, A.; Park, Y. S.; Lee, Y. J.; Chun, Y. S.; Ha, K.; Yoon, K. B., Polyamines as strong molecular linkers for monolayer assembly of zeolite crystals on flat and curved glass. In *Journal of the American Chemical Society*, 2000; Vol. 122, pp 9308-9309.
125. Choi, S.; Lee, Y.; Park, Y.; Ha, K.; Yoon, K., Monolayer Assembly of Zeolite Crystals on Glass with Fullerene as the Covalent Linker. *Journal of the American Chemical Society* **2000**, 122 (21), 5201-5209.
126. Chun, Y. S.; Ha, K.; Lee, Y. J.; Lee, J. S.; Kim, H. S.; Park, Y. S.; Yoon, K. B., Diisocyanates as novel molecular binders for monolayer assembly of zeolite crystals on glass. In *Chemical Communications*, 2002; pp 1846-1847.
127. Wang, Y.; Li, H.; Liu, B.; Gan, Q.; Dong, Q.; Calzaferri, G., Fabrication of oriented zeolite L monolayer via covalent molecular linkers. *Journal of Solid State Chemistry* **2008**.
128. Zhang, B.; Zhou, M.; Liu, X., Monolayer Assembly of Oriented Zeolite Crystals on α -Al₂O₃ Supported Polymer Thin Films. *Advanced Materials* **2008**, 20 (11), 2183-2189.
129. Cho, G.; Lee, J. S.; Glatzhofer, D. T.; Fung, B. M.; Yuan, W. L.; O'Rear, E. A., Ultra-thin zeolite films through simple self-assembled processes. In *Advanced Materials*, 1999; Vol. 11, pp 497-+.
130. Lee, J.; Meng, L.; Norris, D.; Scriven, L.; Tsapatsis, M., Colloidal Crystal Layers of Hexagonal Nanoplates by Convective Assembly. *Langmuir* **2006**, 22 (12), 5217-5219.
131. Tosheva, L.; Valtchev, V. P.; Mihailova, B.; Doyle, A. M., Zeolite beta films prepared via the langmuir-blodgett technique. In *J Phys Chem C*, 2007; Vol. 111, pp 12052-12057.
132. Lee, G. S.; Lee, Y. J.; Yoon, K. B., Layer-by-Layer Assembly of Zeolite Crystals on Glass with Polyelectrolytes as Ionic Linkers. *JOURNAL-AMERICAN CHEMICAL SOCIETY* **2001**.

133. Cucinotta, F.; Popović, Z.; Weiss, E.; Whitesides, G.; De Cola, L., Microcontact Transfer Printing of Zeolite Monolayers. *Advanced Materials* **2008**, NA-NA.
134. Ha, K.; Seonpark, J.; Sunoh, K.; Zhou, Y.; Sungchun, Y.; Lee, Y. J.; Yoon, K. B., Aligned monolayer assembly of zeolite crystals on platinum, gold, and indium–tin oxide surfaces with molecular linkages. *Micropor Mesopor Mat* **2004**, 72 (1-3), 91-98.
135. Yoon, K., Organization of zeolite microcrystals for production of functional materials. In *Accounts Chem Res*, 2007; Vol. 40, pp 29-40.
136. Lee, J.; Lim, H.; Ha, K.; Cheong, H.; Yoon, K., Facile Monolayer Assembly of Fluorophore-Containing Zeolite Rods in Uniform Orientations for Anisotropic Photoluminescence. *Angew. Chem. Int. Ed.* **2006**, 45 (32), 5288-5292.
137. Guerrero-Martínez, A.; Fibikar, S.; Pastoriza-Santos, I.; Liz-Marzán, L.; De Cola, L., Microcontainers with Fluorescent Anisotropic Zeolite L Cores and Isotropic Silica Shells. *Angew. Chem. Int. Ed.* **2008**, NA-NA.
138. Valtchev, V., Core-shell polystyrene/zeolite A microbeads. *CHEMISTRY OF MATERIALS* **2002**.
139. Wang, X.; Tang, Y.; Wang, Y.; Gao, Z.; Yang, W.; Fu, S., Fabrication of hollow zeolite spheres. *Chemical Communications* **2000**, (21), 2161-2162.
140. Choi, J.; Lai, Z.; Ghosh, S.; Beving, D.; Yan, Y.; Tsapatsis, M., Layer-by-Layer Deposition of Barrier and Permselective c-Oriented-MCM-22/Silica Composite Films. *Ind. Eng. Chem. Res.* **2007**, 46 (22), 7096-7106.
141. Valtchev, V.; Mintova, S., Layer-by-layer preparation of zeolite coatings of nanosized crystals. In *Micropor Mesopor Mat*, 2001; Vol. 43, pp 41-49.
142. Zhou, M.; Liu, X.; Zhang, B.; Zhu, H., Assembly of Oriented Zeolite Monolayers and Thin Films on Polymeric Surfaces via Hydrogen Bonding. *Langmuir* **2008**.
143. Ban, T.; Saito, H.; Naito, M.; Ohya, Y.; Takahashi, Y., Synthesis of zeolite L crystals with different shapes. *Journal of Porous Materials* **2007**, 14 (2), 119-126.
144. Cui, X. L.; Zhao, Q.; Li, Z. Z.; Sun, Z. Y.; Jiang, Z. Y., Cyclic voltammetry as a tool to estimate the effective pore density of an anodic aluminium oxide template. *Nanotechnology* **2007**, 18 (21), -.
145. Li, J. W.; Pfanner, K.; Calzaferri, G., Silver-Zeolite-Modified Electrodes - an Intrazeolite Electron-Transport Mechanism. *Journal of Physical Chemistry* **1995**, 99 (7), 2119-2126.
146. Shaw, B. R.; Creasy, K. E.; Lanczycki, C. J.; Sargeant, J. A.; Tirhado, M., Voltammetric Response of Zeolite-Modified Electrodes. *Journal of the Electrochemical Society* **1988**, 135 (4), 869-876.

147. Schatz, T.; Cook, A. R.; Meisel, D., Charge carrier transfer across the silica nanoparticle/water interface. *Journal of Physical Chemistry B* **1998**, *102* (37), 7225-7230.
148. Zhao, *Functional Materials (Chinese)* **2004**, *35*, 2800.
149. Lodhi, M. A. K., Photovoltaics and hydrogen: Future energy options. *Energy Conversion and Management* **1997**, *38* (18), 1881-1893.
150. Abdel-Aal, H. K.; Al-Naafa, M. A., Prospects of "solar" hydrogen for desert development in the Arab world. *International Journal of Hydrogen Energy* **1998**, *23* (2), 83-88.
151. Serrano, E.; Rus, G.; Garcia-Martinez, J., Nanotechnology for sustainable energy. *Renewable & Sustainable Energy Reviews* **2009**, *13* (9), 2373-2384.
152. Arai, J.; Matsuo, A.; Fujisaki, T.; Ozawa, K., A novel high temperature stable lithium salt (Li₂B₁₂F₁₂) for lithium ion batteries. *Journal of Power Sources* **2009**, *193* (2), 851-854.
153. Ikeya, T.; Iwasaki, M.; Takagi, S.; Sugii, Y.; Yada, M.; Sakabe, T.; Kousaka, E.; Tsuchiya, H.; Kanetsuki, M.; Nasu, H.; Ono, M.; Narisoko, H.; Mita, Y.; Nishiyama, K.; Adachi, K.; Iwahori, T., Collaborative investigation on charging electric-vehicle battery systems for night-time load levelling by Japanese electric power companies. *Journal of Power Sources* **1997**, *69* (1-2), 103-111.
154. John, M. S.; Sammells, A. F., Approach for Cost Effective Positive Electrode Current Collectors in the Lithium-Metal Sulfide Battery. *Journal of The Electrochemical Society* **1979**, *126* (8), C314-C314.
155. Ogihara, T.; Matsuo, H.; Yamanaka, S.; Aikiyo, H., Running Characterization of Light Rail Vehicle Powered by Lithium Ion Battery. *Electrochemistry* **2009**, *77* (11), 956-959.
156. Takei, K.; Terada, N.; Iwahori, T.; Tanaka, T.; Mishima, H.; Takeuchi, K., The 200 V 2 kWh energy storage multicell system with 25 Wh Li/LiV₃O₈ single cells. *Journal of Power Sources* **1997**, *68* (1), 78-81.
157. Whittingham, M. S., Electrical Energy Storage and Intercalation Chemistry. *Science* **1976**, *192* (4244), 1126-1127.
158. Chromik, R.; Beck, F., A quantitative discrimination between reversible Li⁺-insertion and irreversible solvent oxidation at a lithium/manganese-spinel electrode. *Electrochimica Acta* **2000**, *45* (14), 2175-2185.
159. Zukalova, M.; Kalbac, M.; Kavan, L.; Exnar, I.; Graetzel, M., Pseudocapacitive lithium storage in TiO₂(B). *Chemistry of Materials* **2005**, *17* (5), 1248-1255.

160. Ellis, B. L.; Makahnouk, W. R. M.; Makimura, Y.; Toghil, K.; Nazar, L. F., A multifunctional 3.5 V iron-based phosphate cathode for rechargeable batteries. *Nature Materials* **2007**, *6* (10), 749-753.
161. Kang, B.; Ceder, G., Battery materials for ultrafast charging and discharging. *Nature* **2009**, *458* (7235), 190-193.
162. Abruna, H. D.; Matsumoto, F.; Cohen, J. L.; Jin, J.; Roychowdhury, C.; Prochaska, M.; van Dover, R. B.; DiSalvo, F. J.; Kiya, Y.; Henderson, J. C.; Hutchison, G. R., Electrochemical energy generation and storage. Fuel cells and lithium-ion batteries. *Bulletin of the Chemical Society of Japan* **2007**, *80* (10), 1843-1855.
163. Fergus, J. W., Ceramic and polymeric solid electrolytes for lithium-ion batteries. *Journal of Power Sources* **2010**, *195* (15), 4554-4569.
164. Guo, B. K.; Shu, J.; Tang, K.; Bai, Y.; Wang, Z. X.; Chen, L. Q., Nano-Sn/hard carbon composite anode material with high-initial coulombic efficiency. *Journal of Power Sources* **2008**, *177* (1), 205-210.
165. Daniel, C., Materials and processing for lithium-ion batteries. *Jom* **2008**, *60* (9), 43-48.
166. Lee, C. W.; Venkatachalapathy, R.; Prakash, J., A novel flame-retardant additive for lithium batteries. *Electrochem. Solid State Lett.* **2000**, *3* (2), 63-65.
167. Tarascon, J. M.; Armand, M., Issues and challenges facing rechargeable lithium batteries. In *Nature*, 2001; Vol. 414, pp 359-367.
168. Tarascon, M.; Gozdz, A. S.; Schmutz, C.; Shokoohi, F.; Warren, P. C., Performance of Bellcore's plastic rechargeable Li-ion batteries. *Solid State Ionics* **1996**, *86-88*, 49-54.
169. Stallworth, P. E.; Fontanella, J. J.; Wintersgill, M. C.; Scheidler, C. D.; Immel, J. J.; Greenbaum, S. G.; Gozdz, A. S., NMR, DSC and high pressure electrical conductivity studies of liquid and hybrid electrolytes. *Journal of Power Sources* **1999**, *82*, 739-747.
170. Kelly, I. E.; Owen, J. R.; Steele, B. C. H., Poly(Ethylene Oxide) Electrolytes for Operation at near Room-Temperature. *Journal of Power Sources* **1985**, *14* (1-3), 13-21.
171. Agrawal, R. C.; Pandey, G. P., Solid polymer electrolytes: materials designing and all-solid-state battery applications: an overview. *Journal of Physics D-Applied Physics* **2008**, *41* (22), -.
172. Lazzari, M.; Scrosati, B., Cyclable Lithium Organic Electrolyte Cell Based on 2 Intercalation Electrodes. *Journal of The Electrochemical Society* **1980**, *127* (3), 773-774.

173. Nikolic, N. D.; Popov, K. I.; Pavlovic, L. J.; Pavlovic, M. G., The effect of hydrogen codeposition on the morphology of copper electrodeposits. 1. The concept of effective overpotential. *Journal of Electroanalytical Chemistry* **2006**, *588* (1), 88-98.
174. Kelder, E. M.; Jak, M. J. G.; deLange, F.; Schoonman, J., A new ceramic lithium solid electrolyte for rechargeable swing type batteries. *Solid State Ionics* **1996**, *85* (1-4), 285-291.
175. Tatsumisago, M.; Hama, S.; Hayashi, A.; Morimoto, H.; Minami, T., New lithium ion conducting glass-ceramics prepared from mechanochemical Li₂S-P₂S₅ glasses. *Solid State Ionics* **2002**, *154*, 635-640.
176. Tatsumisago, M.; Hayashi, A., Preparation of lithium ion conducting glasses and glass-ceramics for all-solid-state batteries. *Journal of Non-Crystalline Solids* **2008**, *354* (12-13), 1411-1417.
177. Barkey, D.; Muller, R.; Tobias, C., Roughness development in metal electrodeposition. *Journal of The Electrochemical Society* **1989**, *136*, 2199.
178. Gu, W. B.; Wang, C. Y., Thermal-electrochemical modeling of battery systems. *Journal of The Electrochemical Society* **2000**, *147* (8), 2910-2922.
179. Gadjourova, Z.; Andreev, Y. G.; Tunstall, D. P.; Bruce, P. G., Ionic conductivity in crystalline polymer electrolytes. *Nature* **2001**, *412* (6846), 520-523.
180. Doyle, M.; Fuller, T. F.; Newman, J., Modeling of Galvanostatic Charge and Discharge of the Lithium Polymer Insertion Cell. *Journal of The Electrochemical Society* **1993**, *140* (6), 1526-1533.
181. Edman, L.; Doeff, M. M.; Ferry, A.; Kerr, J.; De Jonghe, L. C., Transport properties of the solid polymer electrolyte system P(EO)(n)LiTFSI. *Journal of Physical Chemistry B* **2000**, *104* (15), 3476-3480.
182. Armand, M.; Tarascon, J., Building better batteries. In *Nature*, 2008; Vol. 451, pp 652-657.
183. Li, X.; Cheruvally, G.; Kim, J. K.; Choi, J. W.; Ahn, J. H.; Kim, K. W.; Ahn, H. J., Polymer electrolytes based on an electrospun poly(vinylidene fluoride-co-hexafluoropropylene) membrane for lithium batteries. *Journal of Power Sources* **2007**, *167* (2), 491-498.
184. Monroe, C.; Newman, J., Dendrite growth in lithium/polymer systems - A propagation model for liquid electrolytes under galvanostatic conditions. *Journal of The Electrochemical Society* **2003**, *150* (10), A1377-A1384.
185. González, G.; Rosso, M.; Chassaing, E., Transition between two dendritic growth mechanisms in electrodeposition. *Phys. Rev. E* **2008**, *78* (1), 1-5.

186. Singh, M.; Odusanya, O.; Wilmes, G. M.; Eitouni, H. B.; Gomez, E. D.; Patel, A. J.; Chen, V. L.; Park, M. J.; Fragouli, P.; Iatrou, H.; Hadjichristidis, N.; Cookson, D.; Balsara, N. P., Effect of molecular weight on the mechanical and electrical properties of block copolymer electrolytes. *Macromolecules* **2007**, *40* (13), 4578-4585.
187. Li, Y.; Fedkiw, P. S., Nanocomposite gel electrolytes based on fumed silica for lithium-ion batteries. *Journal of The Electrochemical Society* **2007**, *154* (12), A1140-A1145.
188. Bhattacharyya, A. J.; Tarafdar, S.; Middy, T. R., Effective medium theory for ionic conductivity in polycrystalline solid electrolytes. *Solid State Ionics* **1997**, *95* (3-4), 283-288.
189. Stephan, A. M.; Nahm, K. S., Review on composite polymer electrolytes for lithium batteries. *Polymer* **2006**, *47* (16), 5952-5964.
190. Liu, H. K.; Wang, G. X.; Guo, Z. P.; Wang, J. Z.; Konstantinov, K., The impact of nanomaterials on Li-ion rechargeable batteries. *Journal of New Materials for Electrochemical Systems* **2007**, *10* (2), 101-104.
191. Wang, M. K.; Zhao, F.; Guo, Z. H.; Dong, S. J., Poly(vinylidene fluoride-hexafluoropropylene)/organo-montmorillonite clays nanocomposite lithium polymer electrolytes. *Electrochimica Acta* **2004**, *49* (21), 3595-3602.
192. Aravindan, V.; Vickraman, P., Polyvinylidene fluoride-hexafluoropropylene based nanocomposite polymer electrolytes (NCPE) complexed with $\text{LiPF}_3(\text{CF}_3\text{CF}_2)_3$. *European Polymer Journal* **2007**, *43* (12), 5121-5127.
193. Aravindan, V.; Vickraman, P., A novel gel electrolyte with lithium difluoro(oxalato)borate salt and Sb_2O_3 nanoparticles for lithium ion batteries. *Solid State Sciences* **2007**, *9* (11), 1069-1073.
194. Best, A. S.; Ferry, A.; MacFarlane, D. R.; Forsyth, M., Conductivity in amorphous polyether nanocomposite materials. *Solid State Ionics* **1999**, *126* (3-4), 269-276.
195. Ahn, J. H.; Wang, G. X.; Liu, H. K.; Dou, S. X. In *Nanoparticle-dispersed PEO polymer electrolytes for Li batteries*, 11th International Meeting on Lithium Batteries, Monterey, California, Jun 24-28; Elsevier Science Bv: Monterey, California, 2002; pp 422-426.
196. Croce, F.; Persi, L.; Ronci, F.; Scrosati, B. In *Nanocomposite polymer electrolytes and their impact on the lithium battery technology*, 12th International Conference on Solid State Ionics, Halkidiki, Greece, Jun 06-12; Thrace, G.; Secretariat, R.; Technol, U. P. R. C. A. U.; Thessaloniki, U. T. P. S. P. C. P. E. R. I.; Natl Bank Greece, C. B. G. A. B. G. A.; Brewry Sa, P. P. L. P. C. H. L. B. S. A. G.; George P Vasilopoulos Sa, H. L. E. O. N. R. E.; Soc, H. T. M. D., Eds. Elsevier Science Bv: Halkidiki, Greece, 1999; pp 47-52.

197. Liu, H. J.; Hwang, J. J.; Chen-Yang, Y. W., Effects of organophilic clay on the solvent-maintaining capability, dimensional stability, and electrochemical properties of gel poly(vinylidene fluoride) nanocomposite electrolytes. *Journal of Polymer Science Part a-Polymer Chemistry* **2002**, *40* (22), 3873-3882.
198. Xiong, H. M.; Shen, W. Z.; Wang, Z. D.; Zhang, X.; Xia, Y. Y., Liquid polymer nanocomposites PEGME-SnO₂ and PEGME-TiO₂ prepared through solvothermal methods. *Chemistry of Materials* **2006**, *18* (16), 3850-3854.
199. Krawiec, W.; Scanlon, L. G.; Fellner, J. P.; Vaia, R. A.; Giannelis, E. P., Polymer nanocomposites - a new strategy for synthesizing solid electrolytes for rechargeable lithium batteries. *Journal of Power Sources* **1995**, *54* (2), 310-315.
200. Kim, S.; Park, S. J., Preparation and electrochemical behaviors of polymeric composite electrolytes containing mesoporous silicate fillers. *Electrochimica Acta* **2007**, *52* (11), 3477-3484.
201. Liu, Y.; Lee, J. Y.; Hong, L., In situ preparation of poly(ethylene oxide)-SiO₂ composite polymer electrolytes. *Journal of Power Sources* **2004**, *129* (2), 303-311.
202. Walls, H. J.; Riley, M. W.; Singhal, R. R.; Spontak, R. J.; Fedkiw, P. S.; Khan, S. A., Nanocomposite electrolytes with fumed silica and hectorite clay networks: Passive versus active fillers. *Advanced Functional Materials* **2003**, *13* (9), 710-717.
203. Wen, Z. Y.; Gu, Z. H.; Itoh, T.; Lin, Z. X.; Yamamoto, O. In *An investigation of poly(ethylene oxide)/saponite-based composite electrolytes*, 11th International Meeting on Lithium Batteries, Monterey, California, Jun 24-28; Elsevier Science Bv: Monterey, California, 2002; pp 427-431.
204. Kim, S.; Park, S. J., Interlayer spacing effect of alkylammonium-modified montmorillonite on conducting and mechanical behaviors of polymer composite electrolytes. *Journal of Colloid and Interface Science* **2009**, *332* (1), 145-150.
205. Stephan, A. M.; Kumar, T. P.; Kulandainathan, M. A.; Lakshmi, N. A., Chitin-Incorporated Poly(ethylene oxide)-Based Nanocomposite Electrolytes for Lithium Batteries. *Journal of Physical Chemistry B* **2009**, *113* (7), 1963-1971.
206. Samir, M.; Chazeau, L.; Alloin, F.; Cavaille, J. Y.; Dufresne, A.; Sanchez, J. Y. In *POE-based nanocomposite polymer electrolytes reinforced with cellulose whiskers*, 9th International Symposium on Polymer Electrolytes (ISPE-9), Mragowo, POLAND, Aug 22-27; Pergamon-Elsevier Science Ltd: Mragowo, POLAND, 2004; pp 3897-3903.
207. Schroers, M.; Kokil, A.; Weder, C., Solid polymer electrolytes based on nanocomposites of ethylene oxide-epichlorohydrin copolymers and cellulose whiskers. *Journal of Applied Polymer Science* **2004**, *93* (6), 2883-2888.

208. Xiong, H. M.; Liu, D. P.; Zhang, H.; Chen, J. S., Polyether-grafted SnO₂ nanoparticles designed for solid polymer electrolytes with long-term stability. *Journal of Materials Chemistry* **2004**, *14* (18), 2775-2780.
209. Xiong, H. M.; Wang, Z. D.; Xie, D. P.; Cheng, L.; Xia, Y. Y., Stable polymer electrolytes based on polyether-grafted ZnO nanoparticles for all-solid-state lithium batteries. *Journal of Materials Chemistry* **2006**, *16* (14), 1345-1349.
210. Abraham, K. M.; Jiang, Z.; Carroll, B., Highly conductive PEO-like polymer electrolytes. *Chemistry of Materials* **1997**, *9* (9), 1978-1988.
211. Cheng, C. L.; Wan, C. C.; Wang, Y. Y., Microporous PVdF-HFP based gel polymer electrolytes reinforced by PEGDMA network. *Electrochemistry Communications* **2004**, *6* (6), 531-535.
212. Cho, M.; Seo, H.; Nam, J.; Choi, H.; Koo, J.; Lee, Y., High ionic conductivity and mechanical strength of solid polymer electrolytes based on NBR/ionic liquid and its application to an electrochemical actuator. *Sensors and Actuators B-Chemical* **2007**, *128* (1), 70-74.
213. Gayet, F.; Viau, L.; Leroux, F.; Mabilhe, F.; Monge, S.; Robin, J. J.; Vioux, A., Unique Combination of Mechanical Strength, Thermal Stability, and High Ion Conduction in PMMA-Silica Nanocomposites Containing High Loadings of Ionic Liquid. *Chemistry of Materials* **2009**, *21* (23), 5575-5577.
214. Kang, Y. K.; Cheong, K.; Noh, K. A.; Lee, C.; Seung, D. Y., A study of cross-linked PEO gel polymer electrolytes using bisphenol A ethoxylate diacrylate: ionic conductivity and mechanical properties. *Journal of Power Sources* **2003**, *119*, 432-437.
215. Kweon, J. O.; Noh, S. T., Thermal, thermomechanical, and electrochemical characterization of the organic-inorganic hybrids poly(ethylene oxide) (PEO)-silica and PEO-silica-LiClO₄. *Journal of Applied Polymer Science* **2001**, *81* (10), 2471-2479.
216. Leo, C. J.; Rao, G. V. S.; Chowdari, B. V. R., Studies on plasticized PEO-lithium triflate-ceramic filler composite electrolyte system. *Solid State Ionics* **2002**, *148* (1-2), 159-171.
217. Niitani, T.; Shimada, M.; Kawamura, K.; Dokko, K.; Rho, Y. H.; Kanamura, K., Synthesis of Li⁺ ion conductive PEO-PSt block copolymer electrolyte with microphase separation structure. *Electrochemical and Solid State Letters* **2005**, *8* (8), A385-A388.
218. Patel, M.; Chandrappa, K. G.; Bhattacharyya, A. J., Increasing ionic conductivity and mechanical strength of a plastic electrolyte by inclusion of a polymer. *Electrochimica Acta* **2008**, *54* (2), 209-215.
219. Pitawala, H.; Dissanayake, M.; Seneviratne, V. A., Combined effect of Al₂O₃ nano-fillers and EC plasticizer on ionic conductivity enhancement in the solid polymer electrolyte (PEO)(9)LiTf. *Solid State Ionics* **2007**, *178* (13-14), 885-888.

220. Ren, Z.; Sun, K. N.; Liu, Y. Y.; Zhou, X. L.; Zhang, N. Q.; Zhu, X. D., Polymer electrolytes based on poly(vinylidene fluoride-co-hexafluoropropylene) with crosslinked poly(ethylene glycol) for lithium batteries. *Solid State Ionics* **2009**, *180* (9-10), 693-697.
221. Song, Y. X.; Wu, S. Y.; Jing, X. B.; Sun, J. Z.; Chen, D. L., Thermal, mechanical and ionic conductive behaviour of gamma-radiation induced PEO/PVDF(SIN)-LiClO₄ polymer electrolyte system. *Radiation Physics and Chemistry* **1997**, *49* (5), 541-546.
222. Xi, J. Y.; Qiu, X. P.; Chen, L. Q., PVDF-PEO/ZSM-5 based composite microporous polymer electrolyte with novel pore configuration and ionic conductivity. *Solid State Ionics* **2006**, *177* (7-8), 709-713.